

Assessment of coronary flow reserve using a combination of planar first-pass angiography and myocardial SPECT: Comparison with myocardial ^{15}O -water PET

Naoko Nose ^{a,b}, Kazuhito Fukushima ^c, Constantin Lapa ^a, Rudolf A. Werner ^{a,b}, Mehrbod Som Javadi ^d, Junichi Taki ^e, Takahiro Higuchi ^{a,c,f,*}

^a Department of Nuclear Medicine, University Hospital Wuerzburg, Wuerzburg, Germany

^b Comprehensive Heart Failure Center, University Hospital Wuerzburg, Wuerzburg, Germany

^c Division of Nuclear Medicine, Hyogo College of Medicine, Hyogo, Japan

^d Department of Radiology, Johns Hopkins Medical Institution, MD, USA

^e Department of Nuclear Medicine, Kanazawa Graduate University of Medical Sciences, Ishikawa, Japan

^f Kanazawa Cardiovascular Hospital, Ishikawa, Japan

1. Introduction

Coronary flow reserve (CFR), defined as the ratio of increase in coronary blood flow from baseline resting blood flow, is one of the most sensitive parameters to detect early signs of coronary arteriosclerosis [1–8]. Myocardial perfusion PET is a well-established technology for the CFR measurement, however, availability is still limited due its cost [9–11]. Myocardial perfusion SPECT imaging using Tc-99m labeled tracers is one of the most widely available and well-established clinical approaches for detecting myocardial perfusion abnormalities in

patients with ischemic heart disease [12–19]. However, quantification of myocardial flow is challenging due to limited temporal and spatial resolution, attenuation and scatter artifacts.

We have recently proposed a novel approach for the assessment of myocardial flow responses during pharmacological vasodilation stress using a combination of cardiac first pass dynamic planar imaging during tracer administration and subsequent myocardial SPECT [20,21]. In order to compensate for the limitation of temporal resolution of SPECT technology, a dynamic planar angiography is used for tracer input estimation [22]. Separate SPECT imaging serves for local tracer determination. Using the same alignment of scanner and patient positions for both baseline rest and stress scans, effects of attenuation, scatter and partial volume remain the same. Therefore, when calculating a “ratio” between baseline and stress, intrinsic factors of artifacts such as attenuation can be ruled out.

* Corresponding author at: Dept. of Nuclear Medicine, University Hospital Wuerzburg, Oberduerrbacher Str. 6, D-97080 Wuerzburg, Germany.
E-mail address: thiguchi@me.com (T. Higuchi).

In this study, we aimed to further elucidate the feasibility to measure CFR by a combination of dynamic first-pass planar imaging and SPECT in comparison with CFR as assessed by ^{15}O -water PET.

2. Materials and methods

2.1. Patients

The study population consisted of 10 patients (7 men, 3 women; mean age, 61 ± 8 years), who were referred for scintigraphic assessment of coronary artery disease. Seven patients had a previous myocardial infarction. Both a MIBI CFR study and a PET CFR study were performed within an interval of 5 days. The local hospital review board approved the study protocol and all patients gave informed consent.

2.2. Measurement of CFR by MIBI

Augmented regional MIBI myocardial retention during pharmacological vasodilation was calculated based on a theory previously published [21]. The absolute tracer retention can be described as follows:

$$R = Ct/Sbt \quad (1)$$

where R is the absolute MIBI retention of the tracer, Ct is the true radioactivity of the tracer in the regional myocardium and Sbt is the true time integral of arterial radioactivity concentration.

Secondly, radioactivity in myocardium Ct can be expressed as follows:

$$Ct = k_1 Cm \quad (2)$$

where Cm is the regional myocardial count measured with MIBI SPECT study and k_1 is the correction factor for the SPECT measurement including count rate, attenuation factor, partial volume effects and sensitivity of the gamma camera system.

Thirdly, the integral of arterial radioactivity concentration Sbt can be expressed with the time integral of arterial counts, measured by the first pass angiographic study (Sbm), and the correction factors (k_2) for the first pass imaging, including counting rate, attenuation factor, partial volume effects and sensitivity of the gamma camera system. Then, Sbt can be expressed as follows:

$$Sbt = k_2 Sbm \quad (3)$$

CFR measured by MIBI retention (CFR_{MIBI}) is defined as ratio of tracer retention at stress divided by that at baseline

$$\text{CFR}_{\text{MIBI}} = R_s/R_b \quad (4)$$

where $_b$ indicates baseline and $_s$ indicates during pharmacological stress.

Eq. (4) can be changed as follows: Eq. (5) using Eqs. (1)–(3):

$$\begin{aligned} \text{CFR}_{\text{MIBI}} &= R_s/R_b \\ &= (Ct_s/Sbt_s)/(Ct_b/Sbt_b) \\ &= Ct_s Sbt_b / Ct_b Sbt_s \\ &= k_1 Cm_s k_2 Sbm_s / k_1 Cm_b k_2 Sbm_b \end{aligned} \quad (5)$$

The correction factors (k_1 and k_2) can be crossed out in Eq. (5), because they are specific to the gamma camera system and individual patient, and therefore the same at baseline and at stress. Consequently, the final equation is made up of only parameters measured from the SPECT and first pass angiographic study and appears as follows:

$$\text{CFR}_{\text{MIBI}} = Cm_s Sbm_b / Cm_b Sbm_s \quad (6)$$

2.3. MIBI imaging

MIBI planar angiography and SPECT imaging were performed using a one-day rest-stress imaging protocol, which follows the previously published method [21]. At rest and immediately after bolus injection of 370 MBq MIBI into a vein, first-pass radionuclide angiographic data were obtained from the anterior view each second for 90 s in a 6464 matrix. Forty minutes later, SPECT was performed with a dual-headed gamma camera SPECT system (Millennium VG, GE Medial). Thirty projection images were obtained in a 64°64 matrix over 180 degrees, at a duration of 50 s per view. Tomographic images were reconstructed using a ramp filter with a Butterworth filter (order 10; cutoff frequency, 0.55 cycle/cm). Attenuation correction was not performed.

ATP stress was started immediately after baseline SPECT imaging. ATP was infused at a rate of 0.16 mg/kg/min for 5 min. Three minutes after initiation of the ATP injection, 740 MBq of MIBI were injected as a bolus. Radionuclide angiographic data was obtained in the same manner as for the baseline study with the exception of data acquisition being started 5–10 s before the radionuclide injection in order to obtain data for subtraction of the previously injected radionuclide activity. One hour after the ATP stress, SPECT was repeated.

2.4. MIBI data analysis

Time integral of left ventricular first-pass MIBI counts was obtained as the area under the gamma-variate-fitted time activity curve generated from the left ventricular region of interest (ROI). The ROI was determined during left ventricular tracer passage phase at ATP stress by delineating the edge where the count rate was 40% of the peak left ventricular count rate (Fig. 1 A and B). The same ROI was also used for the baseline study. Time activity curve analysis at ATP stress was performed after subtraction of the remaining activity from the baseline study.

Transaxial SPECT slices were reconstructed to 1.1 cm thickness, then myocardial ROIs were drawn manually at the septal, anterior, lateral and posterior walls on a representative transaxial image (Fig. 1 B). The average myocardial count in each ROI at baseline and ATP stress was measured. The myocardial counts at ATP stress were obtained by subtracting the decay-corrected baseline counts.

2.5. ^{15}O -water PET imaging and data analysis

For PET imaging, a 1400 W-10 PET (Shimadzu Corporation, Kyoto, Japan) scanner was used. The scanner can obtain seven slices at 13 mm intervals with a spatial resolution of 4.5 mm full width at half maximum.

Transmission scans were performed for 10 min using a rotating germanium-68 rod source. Then, ^{15}O -CO PET and dynamic ^{15}O -Water PET at baseline and ATP stress were performed in a 128 × 128 matrix. Patients were asked to breathe ^{15}O -CO gas for 2 min and then a 4 min static scan was performed. Ten minutes were allowed for the decay of ^{15}O -CO before the baseline study was initiated. A total of 740 MBq of ^{15}O -Water was injected intravenously over 2 min and a 20-frame dynamic PET examination was performed for 6 min. Ten minutes were allowed for the decay of ^{15}O -Water after the baseline study and before the ATP stress study was initiated. Three minutes after the start of ATP infusion (0.16 mg/kg/min for 9 min), dynamic image acquisition was performed. All images were reconstructed using a filtered back projection method.

Myocardial ROIs were placed on the same locations as for the MIBI study using a representative transaxial slice (slice thickness of 1.1 cm), which corresponded to the slice selected for the MIBI study (Fig. 1 B). Mean blood flows at the ROIs were calculated using a single compartment model according to the previously published method [23,24]. Then, the myocardial blood flow increase ratio during ATP stress (CFR_{PET}) was calculated as the ratio of myocardial blood flow at ATP stress to that at baseline.

2.6. Statistical analysis

Continuous variables were expressed as mean ± SD. Hemodynamic parameters were compared by a paired *t* test. $P < 0.05$ was considered statistically significant.

3. Results

There were significant increases in heart rates and significant decreases in systolic and diastolic blood pressures at ATP stress in both the MIBI and the ^{15}O -Water PET studies.

We successfully obtained 38 segmental data sets from 10 patients. Two segments were rejected because of difficulties determining the ROI on the myocardium at the area of perfusion defects. CFR_{MIBI} was plotted against CFR_{PET} and is presented in Fig. 1C. CFR_{MIBI} increased in conjunction with CFR_{PET} . This proportional relation hit a plateau as myocardial blood flow increase reached approximately 3-times the level of baseline blood flow.

Furthermore, non-linear fitting based on the modified Crone–Renkin model equation used for myocardial perfusion tracer net extractions and myocardial blood flow was applied in our results [25–27]. A good curved correlation between the MIBI retention increase and myocardial blood flow increase was achieved as follows; $Y = 1.40x(1 - \exp(-1.79/x))$ ($r = 0.84$) ($Y = \text{CFR}_{\text{MIBI}}$, $X = \text{CFR}_{\text{PET}}$).

4. Discussion

We described the relationship between CFR as assessed by ^{15}O -Water PET and by a combination of dynamic planar and SPECT imaging studies. As CFR_{PET} increased, CFR_{MIBI} concordantly increased linearly in low flow range. This relation reached a plateau at >3 CFR which might be attributed to reduced MIBI extraction at high coronary flow rates [28–32].

Quantification of absolute flow with SPECT imaging is challenging because of time resolution, scatter, attenuation and partial volume effects. For the measurement of CFR with perfusion SPECT, we performed a combination of planar first-pass angiographic imaging and SPECT

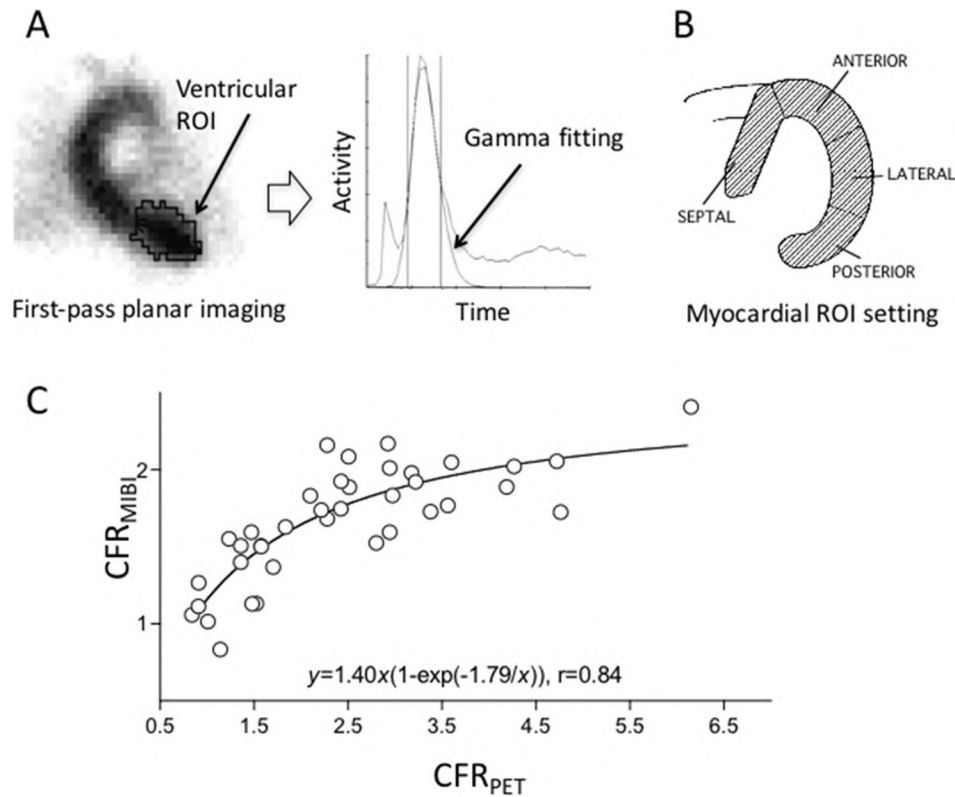


Fig. 1. MIBI first pass planar angiography and subsequent SPECT imaging were performed. (A) First-pass radionuclide angiographic data were obtained from the anterior view. Time integral of left ventricular first-pass MIBI counts was obtained as the area under the gamma-variate-fitted time activity curve generated from the anterior region of interest (ROI). (B) Myocardial ROIs were drawn manually at the septal, anterior, lateral and posterior walls on a representative transaxial image for both MIBI SPECT and ^{15}O -water PET. (C) Relationship between the coronary flow reserve measured by MIBI SPECT (CFR_{MIBI}) and CFR measured by myocardial ^{15}O -water PET (CFR_{PET}). Increase CFR_{MIBI} rose in conjunction with CFR_{PET} , but reached a plateau at higher CFR_{PET} . Solid line indicates non-linear fitted curve.

acquisition [21]. Arterial input function and regional tissue tracer concentrations are required for the measurement of CFR. Especially, estimation of arterial input function is difficult using SPECT due to the limited temporal resolution [20]. Therefore, we employed first-pass planar imaging that has a higher temporal resolution [22]. In general, it is difficult to assess the true counts of an object with a gamma camera requiring corrections for scatter, attenuation and partial volume effects. However, using the same alignment of patient positions at rest and stress, these factors remain specific for both the camera system and the patient. Therefore, whenever possible, identical alignment between patient and detectors is very important in this method.

There are a few reports about CFR assessed by SPECT and validated by PET quantification [33,34]. Consistent with our results, the potential feasibility of SPECT CFR measurement could be demonstrated using a similar approach of first pass planar and SPECT imaging. In comparison, our study mainly differs in the protocol design of the MIBI study. We chose a one-day, rest-stress protocol while the other groups used two-day protocols. In order to avoid the influence of residual tracer activity, we subtracted the previously injected activity from the stress count rates.

5. Conclusions

CFR_{MIBI} equally reflects myocardial blood flow increase from baseline to pharmacological vasodilation as assessed by ^{15}O -Water PET. However, it underestimates flow reserve at high coronary blood flows, most likely due to the pharmacokinetic tracer characteristics of MIBI.

Conflict of interest

The authors report no relationships that could be construed as a conflict of interest.

Disclosure

Part of this work was supported by the Competence Network of Heart Failure funded by the Integrated Research and Treatment Center (IFB) of the Federal Ministry of Education and Research (BMBF) and German Research Council (DFG grant HI 1789/2-1).

References

- [1] H. Oflaz, R. Kurt, A. Cimen, A. Elitok, I. Onur, E. Golcuk, M. Demirturk, S. Batmaz, E. Kasikcioglu, Coronary flow reserve is also impaired in patients with subclinical hypothyroidism, *Int. J. Cardiol.* 120 (2007) 414–416.
- [2] A.C. Rodrigues, C. Frimm Cde, F. Bacal, V. Andreolli, J.M. Tsutsui, E.A. Bocchi, W. Mathias Jr., S.G. Lage, Coronary flow reserve impairment predicts cardiac events in heart transplant patients with preserved left ventricular function, *Int. J. Cardiol.* 103 (2005) 201–206.
- [3] P.L. Van Herck, B.P. Paelinck, S.E. Haine, M.J. Claeys, H. Miljoen, J.M. Bosmans, P.M. Parizel, C.J. Vrints, Impaired coronary flow reserve after a recent myocardial infarction: correlation with infarct size and extent of microvascular obstruction, *Int. J. Cardiol.* 167 (2013) 351–356.
- [4] K. Fukushima, M.S. Javadi, T. Higuchi, P.E. Bravo, D. Chien, R. Lautamaki, J. Merrill, S.G. Nekolla, F.M. Bengel, Impaired global myocardial flow dynamics despite normal left ventricular function and regional perfusion in chronic kidney disease: a quantitative analysis of clinical ^{82}Rb PET/CT studies, *J. Nucl. Med.* 53 (2012) 887–893.
- [5] K. Fukushima, M.S. Javadi, T. Higuchi, R. Lautamaki, J. Merrill, S.G. Nekolla, F.M. Bengel, Prediction of short-term cardiovascular events using quantification of global myocardial flow reserve in patients referred for clinical ^{82}Rb PET perfusion imaging, *J. Nucl. Med.* 52 (2011) 726–732.

- [6] T. Higuchi, C. Abletshausner, S.G. Nekolla, M. Schwaiger, F.M. Bengel, Effect of the angiotensin receptor blocker Valsartan on coronary microvascular flow reserve in moderately hypertensive patients with stable coronary artery disease, *Microcirculation* 14 (2007) 805–812.
- [7] B.C. Zhang, Z.W. Zhou, C. Wang, Y.F. Ma, W.H. Li, D.Y. Li, Fractional flow reserve improves long-term clinical outcomes in patients receiving drug-eluting stent implantation: insights from a meta-analysis of 14,327 patients, *Int. J. Cardiol.* 177 (2014) 1044–1048.
- [8] H.J. Youn, C.S. Park, E.J. Cho, H.O. Jung, H.K. Jeon, J.M. Lee, Y.S. Oh, W.S. Chung, J.H. Kim, K.B. Choi, S.J. Hong, Pattern of exercise-induced ST change is related to coronary flow reserve in patients with chest pain and normal coronary angiogram, *Int. J. Cardiol.* 101 (2005) 299–304.
- [9] M. Fiechter, C. Gebhard, J.R. Ghadri, T.A. Fuchs, A.P. Pazhenkottil, R.N. Nkoulou, B.A. Herzog, U. Altorfer, O. Gaemperli, P.A. Kaufmann, Myocardial perfusion imaging with ¹³N-ammonia PET is a strong predictor for outcome, *Int. J. Cardiol.* 167 (2013) 1023–1026.
- [10] C. Anagnostopoulos, A. Georgakopoulos, N. Pianou, S.G. Nekolla, Assessment of myocardial perfusion and viability by positron emission tomography, *Int. J. Cardiol.* 167 (2013) 1737–1749.
- [11] B.E. Sobel, S.R. Bergmann, Cardiac positron emission tomography, *Int. J. Cardiol.* 2 (1982) 273–277.
- [12] C.C. Lin, H.J. Ding, Y.W. Chen, J.J. Wang, S.T. Ho, A. Kao, Usefulness of technetium-99m sestamibi myocardial perfusion SPECT in detection of cardiovascular involvement in patients with systemic lupus erythematosus or systemic sclerosis, *Int. J. Cardiol.* 92 (2003) 157–161.
- [13] T.F. Christian, R.J. Gibbons, Myocardial perfusion imaging in myocardial infarction and unstable angina, *Cardiol. Clin.* 12 (1994) 247–260.
- [14] P. Kailasath, A.J. Sinusas, Technetium-99m-labeled myocardial perfusion agents: are they better than thallium-201? *Cardiol. Rev.* 9 (2001) 160–172.
- [15] M.R. Mansoor, G.V. Heller, Recent developments in the prognostic use of myocardial perfusion imaging, *Curr. Opin. Cardiol.* 12 (1997) 571–580.
- [16] H.G. Stratmann, B.R. Tamesis, L.T. Younis, M.D. Wittry, D.D. Miller, Prognostic value of dipyridamole technetium-99m sestamibi myocardial tomography in patients with stable chest pain who are unable to exercise, *Am. J. Cardiol.* 73 (1994) 647–652.
- [17] D.A. Calnon, P.D. McGrath, A.L. Doss, F.E. Harrell Jr., D.D. Watson, G.A. Beller, Prognostic value of dobutamine stress technetium-99m-sestamibi single-photon emission computed tomography myocardial perfusion imaging: stratification of a high-risk population, *J. Am. Coll. Cardiol.* 38 (2001) 1511–1517.
- [18] N. Tamaki, Y. Kuge, E. Tsukamoto, Clinical roles of perfusion and metabolic imaging, *J. Cardiol.* 37 (Suppl. 1) (2001) 57–64.
- [19] R.S. Lima, A. De Lorenzo, M.R. Pantoja, A. Siqueira, Incremental prognostic value of myocardial perfusion 99m-technetium-sestamibi SPECT in the elderly, *Int. J. Cardiol.* 93 (2004) 137–143.
- [20] S.G. Nekolla, C. Rischpler, K. Nakajima, Myocardial blood flow quantification with SPECT and conventional tracers: a critical appraisal, *J. Nucl. Cardiol.* 21 (2014) 1089–1091.
- [21] J. Taki, S. Fujino, K. Nakajima, I. Matsunari, H. Okazaki, T. Saga, H. Bunko, N. Tonami, (^{99m}Tc)-sestamibi retention characteristics during pharmacologic hyperemia in human myocardium: comparison with coronary flow reserve measured by Doppler flowire, *J. Nucl. Med.* 42 (2001) 1457–1463.
- [22] J.L. Caplin, D.S. Dymond, W.D. Flatman, J.C. O'Keefe, R.A. Spurrell, The adequacy of radioisotope mixing from bolus injections in first-pass radionuclide angiographic assessment of right ventricular function: a study using gold-195m, *Int. J. Cardiol.* 12 (1986) 185–192.
- [23] H. Iida, I. Yokoyama, D. Agostini, T. Banno, T. Kato, K. Ito, Y. Kuwabara, Y. Oda, T. Otake, Y. Tamura, E. Tadamura, T. Yoshida, N. Tamaki, Quantitative assessment of regional myocardial blood flow using oxygen-15-labelled water and positron emission tomography: a multicentre evaluation in Japan, *Eur. J. Nucl. Med.* 27 (2000) 192–201.
- [24] H. Laine, O.T. Raitakari, H. Niinikoski, O.P. Pitkanen, H. Iida, J. Viikari, P. Nuutila, J. Knuuti, Early impairment of coronary flow reserve in young men with borderline hypertension, *J. Am. Coll. Cardiol.* 32 (1998) 147–153.
- [25] H.R. Schelbert, M.E. Phelps, S.C. Huang, N.S. MacDonald, H. Hansen, C. Selin, D.E. Kuhl, N-13 ammonia as an indicator of myocardial blood flow, *Circulation* 63 (1981) 1259–1272.
- [26] N.A. Mullani, R.A. Goldstein, K.L. Gould, S.K. Marani, D.J. Fisher, H.A. O'Brien Jr., M.D. Loberg, Myocardial perfusion with rubidium-82. I. Measurement of extraction fraction and flow with external detectors, *J. Nucl. Med.* 24 (1983) 898–906.
- [27] C.A. Nienaber, O. Ratib, S.S. Gambhir, J. Krivokapich, S.C. Huang, M.E. Phelps, H.R. Schelbert, A quantitative index of regional blood flow in canine myocardium derived noninvasively with N-13 ammonia and dynamic positron emission tomography, *J. Am. Coll. Cardiol.* 17 (1991) 260–269.
- [28] P.G. Melon, R.S. Beanlands, T.R. DeGrado, N. Nguyen, N.A. Petry, M. Schwaiger, Comparison of technetium-99m sestamibi and thallium-201 retention characteristics in canine myocardium, *J. Am. Coll. Cardiol.* 20 (1992) 1277–1283.
- [29] I. Matsunari, F. Haas, N.T. Nguyen, G. Reidel, I. Wolf, R. Senekowitsch-Schmidtke, G. Stocklin, M. Schwaiger, Comparison of sestamibi, tetrofosmin, and Q12 retention in porcine myocardium, *J. Nucl. Med.* 42 (2001) 818–823.
- [30] D.K. Glover, R.D. Okada, Myocardial technetium 99m sestamibi kinetics after reperfusion in a canine model, *Am. Heart J.* 125 (1993) 657–666.
- [31] D.K. Glover, R.D. Okada, Myocardial kinetics of Tc-MIBI in canine myocardium after dipyridamole, *Circulation* 81 (1990) 628–637.
- [32] D.K. Glover, M. Ruiz, N.C. Edwards, M. Cunningham, J.P. Simanis, W.H. Smith, D.D. Watson, G.A. Beller, Comparison between ²⁰¹Tl and ^{99m}Tc sestamibi uptake during adenosine-induced vasodilation as a function of coronary stenosis severity, *Circulation* 91 (1995) 813–820.
- [33] Y. Ito, C. Katoh, K. Noriyasu, Y. Kuge, H. Furuyama, K. Morita, T. Kohya, A. Kitabatake, N. Tamaki, Estimation of myocardial blood flow and myocardial flow reserve by ^{99m}Tc-sestamibi imaging: comparison with the results of [¹⁵O]H₂O PET, *Eur. J. Nucl. Med. Mol. Imaging* 30 (2003) 281–287.
- [34] T. Tsukamoto, Y. Ito, K. Noriyasu, K. Morita, C. Katoh, H. Okamoto, N. Tamaki, Quantitative assessment of regional myocardial flow reserve using tc-99m-sestamibi imaging, *Circ. J.* 69 (2005) 188–193.